Eur. Radiol. 8, 1123–1129 (1998)

European
Radiology

Original article

Human articular cartilage: in vitro correlation of MRI and histologic findings

M. Uhl[1], **Ch. Ihling**[2], **K. H. Allmann**[1], **J. Laubenberger**[1], **U. Tauer**[2], **C. P. Adler**[2], **M. Langer**[1]

[1] Department of Diagnostic Radiology, University Hospital of Freiburg, Hugstetter-Strasse 55, D-79106 Freiburg, Germany
[2] Department of Pathology, University Hospital of Freiburg, Hugstetter-Strasse 55, D-79106 Freiburg, Germany

Received 13 February 1997; Revision received 27 June 1997; Accepted 29 December 1997

Abstract. The aim of our study was to correlate MRI with histologic findings in normal and degenerative cartilage. Twenty-two human knees derived from patients undergoing amputation were examined with 1.0- and 1.5-T MR imaging units. Firstly, we optimized two fat-suppressed 3D gradient-echo sequences. In this pilot study two knees were examined with fast imaging with steady precession (FISP) sequences and fast low-angle shot (FLASH, SPGR) sequence by varying the flip angles (40, 60, 90°) and combining each flip angle with different echo time (7, 10 or 11, 20 ms). We chose the sequences with the best visual contrast between the cartilage layers and the best measured contrast-to-noise ratio between cartilage and bone marrow. Therefore, we used a 3D FLASH fat-saturated sequence (TR/TE/flip angle = 50/11 ms/40°) and a 3D FISP fat-saturated sequence (TR/TE/flip angle = 40/10 ms/40°) for cartilage imaging in 22 human knees. The images were obtained at various angles of the patellar cartilage in relation to the main magnetic field (0, 55, 90°). The MR appearances were classified into five categories: normal, intracartilaginous signal changes, diffuse thinning (cartilage thickness < 3 mm), superficial erosions, and cartilage ulcers. After imaging, the knees were examined macroscopically and photographed. In addition, we performed histologic studies using light microscopy with several different stainings, polarization, and dark field microscopy as well as electron microscopy. The structural characteristics with the cartilage lesions were correlated with the MR findings. We identified a hyperintense superficial zone in the MR image which did not correlate to the histologically identifiable superficial zone. The second lamina was hypointense on MRI and correlated to the bulk of the radial zone. The third (or deep) cartilage lamina in the MR image seemed to represent the combination of the lowest portion of the radial zone and the calcified cartilage. The width of the hypointense second zone correlated weakly to the accumulation of proteoglycans in the radial zone. The trilaminar MRI appearance of the cartilage was only visible when the cartilage was thicker than 2 mm. In cartilage degeneration, we found either a diffuse thinning of all layers or circumscribed lesions ("cartilage ulcer") of these cartilage layers in the MR images. Early cartilage degeneration was indicated by a signal loss in the superficial zone, correlating to the histologically proven damage of proteoglycans in the transitional and radial zone along with destruction of the superficial zone. We found a strong effect of cartilage rotation in the main magnetic field, too. A rotation of the cartilage structures caused considerable variation in the signal intensity of the second lamina. Cartilage segments in a 55°angle to the magnetic main field had a homogeneous appearance, not a trilaminar appearance. The signal behavior of hyaline articular cartilage does not reflect the laminar histologic structure. Osteoarthrosis and cartilage degeneration are visible on MR images as intracartilaginous signal changes, superficial erosions, diffuse cartilage thinning, and cartilage ulceration.

Key words: MRI – Articular cartilage – Histology – Osteoarthritis

Correspondence to: M. Uhl

Introduction

Magnetic resonance imaging holds great promise in the noninvasive accurate detection of chondral lesions. It offers a superior soft tissue contrast, has multiplanar capability, and permits the direct visualization of articular cartilage [1, 2]. On MR images the normal articular cartilage has a zonal appearance. Lehner et al. [3] found two separate zones of cartilage with varying T1 and T2 relaxation times and postulated this bilaminar appearance to be related to differing water concentrations in the various layers. Modl et al. [4], in a study of whole joints, further de-

scribed a trilaminar appearance and tried to correlate these layers with different histologic layers of cartilage. They postulated the varying appearance of the different layers to be secondary to magnetic susceptibility effects rather than to differing water concentrations. Rubenstein et al. [5] tried to clarify the trilaminar appearance of cartilage. By imaging bovine patellas at various angles in relation to the main magnetic field, they found that cartilage had different appearances depending on these angles. Articular cartilage had a trilaminar appearance that was most striking at 0 and 90° positions. Erickson et al. [6] postulated a truncation artifact rather than a zonal differentiation of histologic anatomy as the underlying cause of the laminar appearance.

Rubenstein et al. [7] investigated the effects of compression and recovery on bovine articular cartilage. The varying appearance and signal intensity characteristics of cartilage under pressure are hypothesized to result from a combination of net water loss and reorientation of collagen structure. A laminar appearance on spin-echo (SE) images at 1.5 T was described by these authors (TR/TE = 800/33 ms). The laminae were named L1 (low-signal-intensity line on the interface between two adjacent cartilage segments), L2 (superficial lamina with high intensity), L3 (middle lamina of low signal), L4 (deep lamina of intermediate signal intensity, and L5 (hypointense zone of calcified cartilage).

The purpose of the present study was to optimize the MR variables for best visualization of the internal architecture of the hyaline cartilage (in vitro study), and to correlate the MRI appearance of these cartilage layers with the histologic layers. We intended particularly to investigate the differences between normal and degenerated human hyaline cartilage.

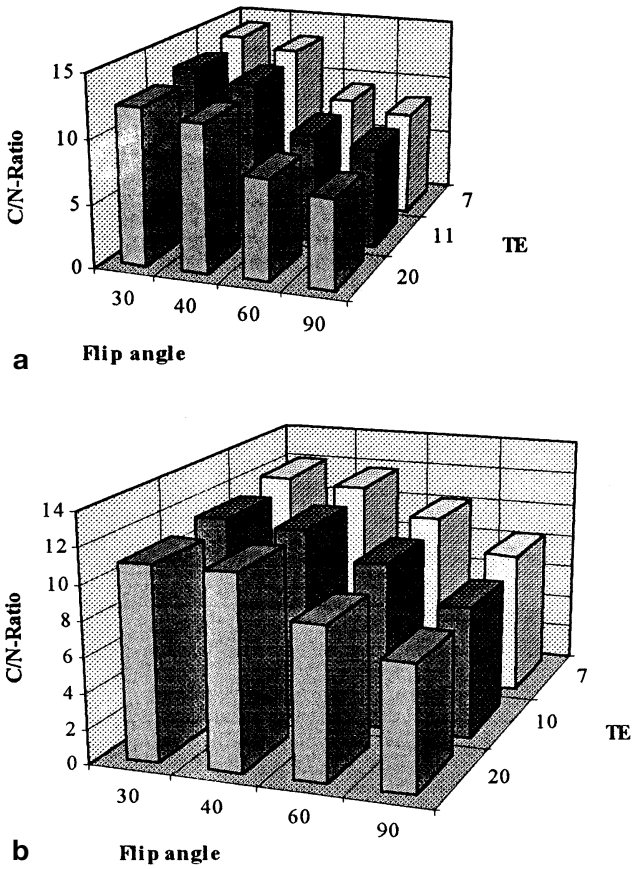

Fig. 1 a, b. Contrast-to-noise ratio (cartilage/bone marrow) in two patellas. **a** FLASH sequences and **b** FISP sequences

Materials and methods

Twenty-two human knees (patient age range 50–72 years) derived from patients undergoing amputation for severe occlusive atherosclerosis with clinical complications, e.g., gangrene were examined with 1.0-T (all knees) and 1.5-T (two knees) imaging units (Magnetom Impact Expert, and Vision, Siemens, Erlangen, Germany), using a commercial knee coil.

Pilot study

The optimization of the gradient-echo sequences [fast low-angle shot (FLASH), SPGR], [fast imaging with steady precession (FISP), SSFP] was achieved by imaging two knees with varying flip angles of both gradient-echo techniques (30, 40, 60, 90°) and combined each flip angle with a different TE (7, 10 or 11, or 20 ms) to yield a total of 16 different imaging sequences for each gradient-echo sequence. Both types of sequences had a 3D data acquisition and were fat-suppressed techniques. The images were obtained at various angles of the patellar cartilage in relation to the main magnetic field (0, 55, 90°). The patellar cartilage was moved from a coronal to a sagittal position in relation to the main magnetic field. The signal intensity of the different cartilage layers were compared visually by two experienced radiologists by consensus. We chose the sequences with the optimal contrast-to-noise ratios between the cartilage and the adjacent bone marrow (condyle; Fig. 1). Contrast-to-noise ratios for cartilage vs bone marrow were calculated as the signal of intensity of cartilage minus the signal intensity of marrow divided by the standard deviation of noise. In addition, images were subjectively evaluated by two of the authors regarding the visualization of cartilage structure and internal detail.

Actual study

All knees were examined with the sequences determined by the pilot study:

1. 3D FLASH fat-saturated sequence (TR/TE/flip angle = 50/11 ms/40°)
2. 3D FISP fat-saturated sequence (TR/TE/flip angle = 40/10 ms/40°).

In addition, we used the following sequences:

1. T2-weighted fast spin-echo sequence (FSE; TR/TE = 4500/120 ms; echo train length = 7)

2. T1-weighted SE sequence (TR/TE = 550/14 ms)

We obtained sagittal and transverse sections with 1.5-mm (FISP and FLASH sequences) and 3-mm (SE and FSE sequences) slice thickness. The imaging matrix was 360×256, 14-cm field of view, and two signal averages in all sequences. The frequency encoding was anterior–posterior. The patellar surface stood perpendicular to the main magnetic field B_o. To exclude truncation artifacts as a cause of trilaminar appearance of cartilage, we repeated the FLASH fat-saturated sequence with a different matrix (512×512) in two knees.

The thickness of the individual layers in the trilaminar MR image of the retropatellar cartilage (superficial zone with high signal intensity, middle zone with low signal intensity, and a deep layer with high signal intensity; see Fig. 4) was measured. The MRI appearances of the cartilage were classified into five categories: normal, intracartilaginous signal changes, diffuse thinning (cartilage thickness < 3 mm), superficial erosions, and cartilage ulcers (lesions deeper than 2.5 mm).

After MR imaging, all knees were examined macroscopically and photographed. Furthermore, 16 knees were sliced with a band saw in planes corresponding to that of the MR images (8 sagittal, 8 coronal), and the slice thickness was approximately 3 mm. Then, eight specimens of hyaline knee cartilage with intracartilaginous MRI signal inhomogeneities or surface lesions were taken. As control, eight cartilage specimens were investigated from normal-appearing hyaline cartilage in MRI.

The tissue was prepared according to standard histologic methods [8]. Sections were 5 μm thick. Serial sections were stained for hematoxylin-eosin, van Gieson (fibrils), and safranin-O (proteoglycans). With safranin-O staining, proteoglycans and mucin were marked orange to red [8]. Furthermore, dark field microscopy (DFM), polarizing microscopy (PM; six specimens), and transmission electron microscopy (two specimens; CM100, Philips, Eindhoven, The Netherlands) was applied.

For the thickness measurement of the various histologic layers, a morphometric software (AnalySIS, SIS, Münster, Germany) was applied. We correlated in all cases the thickness (percent of the whole cartilage thickness) of the different cartilage layers at MR images and histologic sections at defined cartilage areas (medial joint facet of the patella and corresponding facet of the medial condyle).

Histologically, three zones were measured in the safranin-O stained specimens: The thickness of the superficial layer, of the transitional and middle zone, and of the deep zone. The zones were distinguishable by different grades of safranin coloration [8].

Results

MR findings

On every gradient-echo image, the three zones of normal cartilage were consistently distinguishable on the retropatellar and condylar articular cartilage. The first zone, characterized by high signal, was present at the junction of the cartilage and subchondral bone. The adjacent zone above the first zone had low signal intensity. A third zone, characterized as a band of high signal intensity, was identified at the surface of the cartilage. Joint fluid had an intermediate signal intensity. The thickness of the zones varied from region to region and are listed below.

In all circumscribed chondral lesions of the retropatellar cartilage ("cartilage ulcer"; $n = 7$) the trilaminar appearance was destroyed, whereas in cases of diffuse degenerative thinning of the retropatellar articular cartilage ($n = 11$) their trilaminar appearance was preserved. In very thin-cartilage areas (thickness < 2 mm; $n = 4$) this trilaminar appearance cannot be observed.

The trilaminar appearance did not seem to be related to a chemical shift artifact, as it did not change in appearance when the phase and frequency directions were exchanged or the strength of the magnetic main field increased (1.0–1.5 T). There was no hint that the trilaminar appearance was due to a susceptibility effect, as the layers appeared equally well on spin-echo and gradient-echo sequences. We did not find a change in the trilaminar cartilage appearance by increasing the number of phase-encoding steps (matrix size 512×512, FLASH fat-saturated sequence). Therefore, a truncation artifact seems not to be related to the trilaminar appearance of the cartilage.

The variation of the angles between the cartilage and the main magnetic field had a strong influence on the appearance of the cartilage layers. At the 55° position we found a homogeneous appearance. At the 0 and 90° position a remarkable trilaminar appearance was visible. In areas with very thin cartilage ($n = 4$) or cartilage ulcers ($n = 7$), the trilaminar appearance was absent in every cartilage orientation.

Light microscopic findings

As shown by PM techniques in normal articular cartilage, we found a superficial zone with compact tangentially orientated collagen fibrils (type-II collagen). Safranin-O-staining was absent in this zone.

The transitional zone, immediately below the superficial zone, displayed weak safranin-O staining, indicating the presence of small amounts of proteoglycans. There was only a loose mesh of collagen fibrils. The deep radial zone contained collagen fibrils oriented perpendicularly to the surface of the cartilage and a big amount of proteoglycans. The deepest zone adjacent to the cortical bone showed only weak safranin-O-staining.

All of the eight histologic sections of the hyaline cartilage with the MRI diagnosis of cartilage ulcers, small surface lesions, or intracartilaginous signal changes demonstrated histologically complete loss of the superficial zone. The collagen fibrils of the radial zone were aligned perpendicularly to the surface like a "shaving

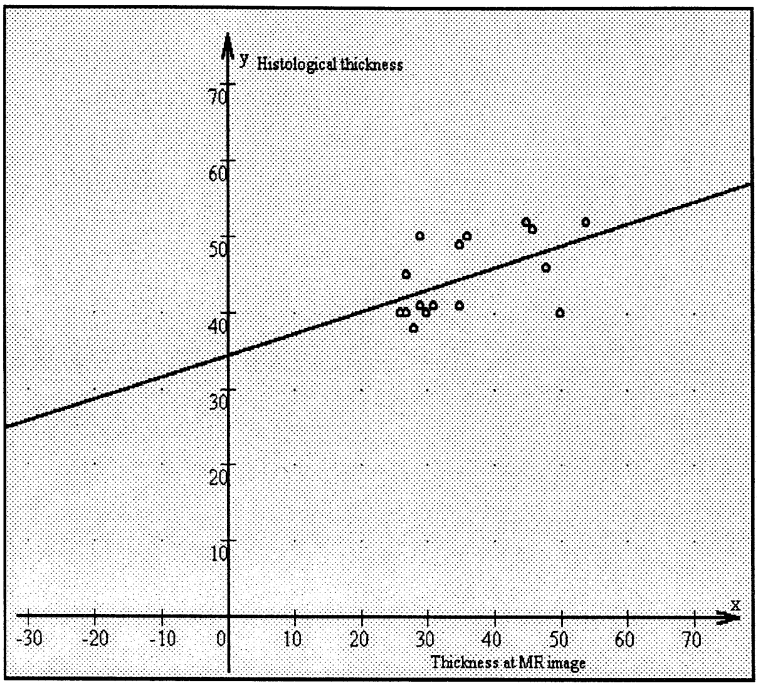

Fig. 2. Correlation of MR image and histology of cartilage thickness: thickness of the middle zone (MR image of cartilage; *x*-axis) and thickness of the radiate zone (cartilage histology; *y*-axis); $n = 16$ cartilage areas, linear correlation coefficient = 0.52. The distribution of proteoglycans in the radial zone (safranin-O pos.) correlates not exactly with the middle zone at MR image of cartilage

brush" and reached the surface of the cartilage. Deep ulcers ($n = 3$) reached the deep radiate zone or even the subchondral cortical bone.

Five cartilage areas with normal MR thickness of the cartilage, but intracartilaginous signal changes (loss of signal intensity in fat-saturated FLASH or FISP sequences), were examined histologically. All showed early degenerative cartilage changes with loss of proteoglycans in the transitional and radial zone along with destruction of the cartilage surface (superficial zone; see Fig. 6 a)

Electronmicroscopy (EM) findings

Transmission electronmicroscopy (EM) visualized the architecture and the arrangement of the collagen fibrils. In the normal superficial tangential zone, the fibrils were arranged parallel to the articular surface. In the normal transitional zone and radial zone, we found a meshwork of fibrils with a predominantly oblique arrangement. In the deep zone a perpendicular arrangement of the loose fiber bundles was found.

Correlation of different cartilage layer thickness at MRI and histology

On MR images of the central retropatellar cartilage (FLASH sequence), the deep zone occupied an average of 10–56 %, the middle zone an average of 26–54 %, and the superficial zone occupied an average of 10–40 % of the whole cartilage thickness.

At histology (hematoxylin and eosin, safranin-O) the average thickness of the calcified cartilage-zone cartilage layer was 10–15 %, of the radial and transitional zone 40–85 %, and of the superficial cartilage layer 5–12 % of the whole cartilage thickness.

Intraindividual correlation at the defined cartilage areas showed no relation between the thickness of the middle zone visible on MRI and the histologic safranin-O-positive radial zone visible in safranin-O-stained sections (Figs. 2, 3). The correlation was also not better in normal cartilage status (Fig. 4).

Discussion

One part of the present study was designed to correlate histologic zones of hyaline cartilage with cartilage structures seen in MRI. The MR appearance of articular cartilage is laminated, although apparent disagreement exists about the number and signal intensity characteristics of the laminae [7]. We found a trilaminar MR appearance of hyaline cartilage, consisting of a high-signal-intensity surface lamina, a middle lamina of intermediate to low signal intensity, and a high-signal-intensity deep lamina (Fig. 4 a) [1, 2, 4]. In contrast, Rubenstein et al. [7] described five laminae, adding a very thin interface line between two articulating cartilage layers, and a hypointense zone of calcified, low-signal cartilage to the mentioned three laminas. This difference in results is probably due to the higher spatial resolution he had.

Normal cartilage has four well-known histologic layers [3, 9, 10, 14, 15]: a superficial zone, a transitional zone, a deep radial zone, and a deep calcified zone. The superficial lamina visible on MR images corresponds in location but not in thickness to the histologic superficial and/or transitional zone. The second zone on MRI corresponds only approximately to the bulk of the radial zone (Fig. 2), whereas the third zone on MRI correlates in location, but never in thickness, to the cal-

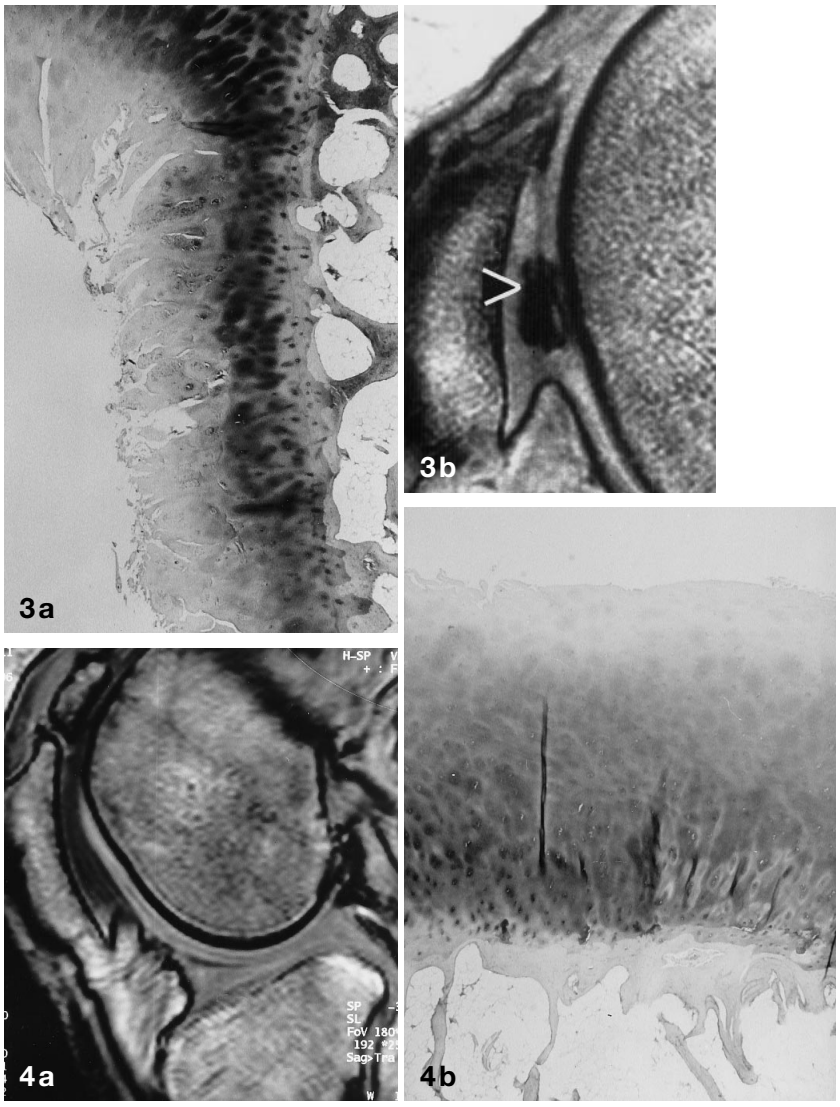

Fig. 3. **a** Histology (safranin-O staining, × 40) of retropatellar cartilage ulcer. Note the trilaminar appearance of the articular cartilage. **b** MR image of this ulcer (3D FLASH, TR/TE/flip angle = 50/11 ms/40°). Cartilage surface and middle zone are circumscribed hypointensely

Fig. 4 a, b. Laminar appearance of normal hyaline cartilage (3D FISP, TR/TE/flip angle = 40/10 ms/40°). **a** Recognize the three zones in the hyaline cartilage of the femur condyle. **b** Histologic correlation: Note the laminar appearance of the condylar cartilage (safranin-O, × 25). There is no correlation between the different histologic layers and the MRI zones

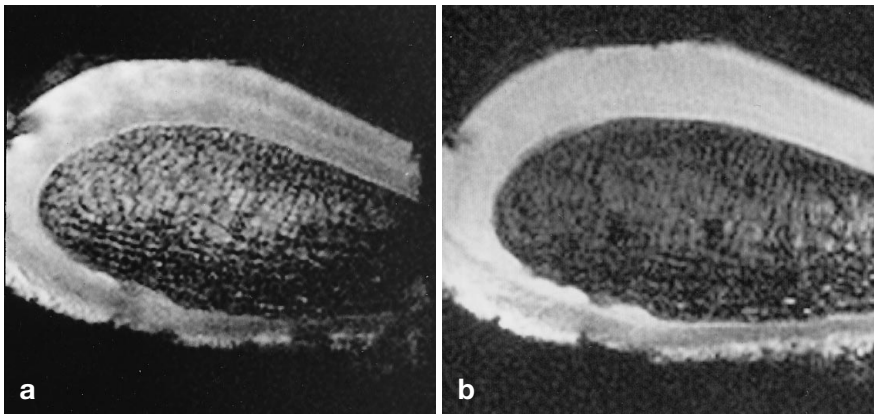

Fig. 5 a, b. Demonstration of orientation effects: images of the same section from an isolated patellar specimen, with a main magnetic field directed toward the top of the images and with the frequency-encoding direction from top to bottom. Note the orientation-dependent appearance of the cartilage layers. Sagittal 3D FLASH fat-saturated sequence (TR/TE/flip angle = 50/11 ms/40°), matrix 512 × 512, field of view 100 mm^2. **a** Patella stood perpendicular to the main magnetic field B_o. Note the zonal appearance of the cartilage. **b** Patella stood oblique (55°) to the main magnetic field. Note the homogeneous appearance of the cartilage

cified zone. Therefore, the results revealed no consistent correlation between the histologic zones and the trilaminar MR appearance of cartilage.

In accordance to Rubenstein et al. [5], we also found a strong effect of cartilage rotation in the main magnetic field. A rotation of the cartilage structures varied considerably the signal intensity of the second lamina. Cartilage segments in a 55° angle to the magnetic field had a homogeneous appearance, not a trilaminar appearance. We hypothesized that the internal collagen structure in the radial zone of cartilage and its orientation influence the signal intensity of the cartilage zones, partic-

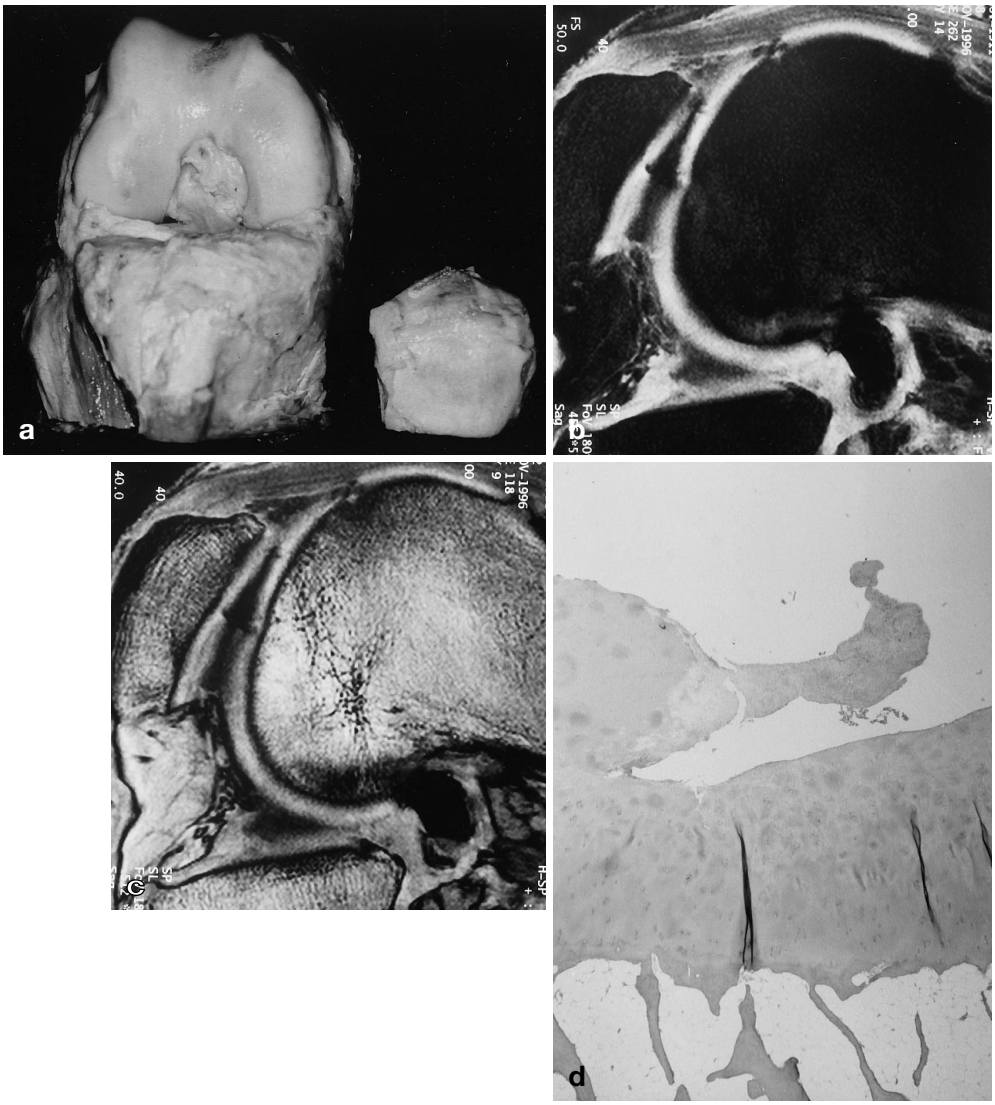

Fig. 6a–d. Osteoarthrosis. **a** Macroscopic cartilage ulcers in the retropatellar cartilage and a circumscribed thinning of the condylar cartilage. **b** MRI correlation in a FLASH sequence (3D fat-saturated FLASH, TR/TE/flip angle = 50/11 ms/40°). **c** A FISP sequence (3D fat-saturated FISP, TR/TE/flip angle = 40/10 ms/40°). Note the retropatellar cartilage lesion and the absent trilaminar appearance of the whole cartilage. Histology (hematoxylin and eosin, × 10) of the patellar cartilage. Note the disrupted margin of the ulcer

ularly from the second lamina with its radially orientated collagen fibers. As first described by Rubenstein et al. [5], the orientation-dependent T2 of collagen fibers in cartilage is the critical determinant of signal intensity. He attributed this phenomena to the restricted motion of water molecules parallel to the direction of collagen fibers. Spin–spin coupling (T2) between two adjacent protons are mediated by the magnetic dipolar fields of each proton. The magnetic dipolar fields are described by the term $(3 \cos^2 \Phi\text{-}1)$, where Φ is the angle between the main magnetic field and a vector through adjacent protons. In the case of freely moving water protons, this angular dependence averages to zero. With the angular orientation of bounded water molecules along the collagen fibers, however, a net angular dependence remains, leading to the "anisotropic T2 effect." The spin–spin coupling is minimized at the angle of $\Phi = 55°$, known as the "magic angle" (direction of the minimum dipolar coupling and maximal T2). This phenomenon is visualized in Fig. 5 (isolated patellar specimen). However, this variation in signal intensities occurred only in cartilage areas with a visible trilaminar appearance (cartilage thicker than 2 mm at least), probably due to partial volume effects.

The second part of our study was designed to correlate the MRI findings of degenerated articular cartilage and histology. The results suggest that both histologically normal and degenerate hyaline cartilage can be distinguished by MRI. Early intracartilaginous degenerative lesions are characterized histologically by a loss of water-binding proteoglycans [10, 11, 14, 17]. The degradation of the intracartilaginous proteoglycans cause a circumscribed signal change resulting in a signal decrease in the MR images [11–14, 17]. In all 5 cases with histologically proven early cartilage degenerations, we found without exception this match of histologically proven loss of proteoglycans in the transitional and radial zone, the destruction of the superficial zone of the cartilage, and the signal decrease in the fat-saturated FLASH and FISP sequences. This MRI signal change was located in the superficial layer. In moderate advanced circumscribed chondral lesions (early cartilage ulcers, histologically deeper than 1–2 mm), a defect in the superficial zone was always visible by MRI. Ad-

vanced chondral lesions showed deep ulcers in all zones of the cartilage with complete absence of the mentioned trilaminar MR cartilage appearance (Fig. 6). Diffuse thinned cartilage areas with a cartilage thickness of less than 3 mm were indicated by the loss of the trilaminar cartilage appearance.

Certain factors prevent an exact correlation between the MR image and the histologic zones. Voxel dimensions in 1.5-mm slices cause partial volume effects. In addition, the border between the different zones undulates. The effect of regional variations in the four zones on sections used in MRI may be different from that on anatomic sections [16, 17]. Exact correlation between MRI and histologic sections therefore cannot be expected. A potential limitation of the present study is the use of amputated knees which were not derived from subjects from a homogenous clinical population.

In summary, MR signal behavior of hyaline articular cartilage only vaguely reflects the laminar histologic structure. Because of its poor correlation between the trilaminar appearance of cartilage on MRI and histologically identified layers, the importance of the trilaminar appearance of hyaline cartilage on MR images remains unclear.

Osteoarthrosis with early intracartilaginous degenerations, superficial erosions, cartilage ulcers, or diffuse thinning of the hyaline cartilage were visible by MRI.

The magic-angle phenomenon influences strongly the presence or absence of the laminar appearance of articular cartilage. The MR appearance of normal cartilage consists of three laminae, yet the cartilage may appear homogeneous at an orientation corresponding to the magic angle of 55°.

References

1. Recht MP, Resnick D (1995) Magnetic resonance imaging of articular cartilage: the state of the art. J Rheumatol (Suppl 43) 22: 52–55
2. Recht MP, Piraino DW, Paletta GA, Schils JP, Belhobek GH (1996) Accuracy of fat-suppressed three-dimensional spoiled gradient-echo FLASH MR imaging in the detection of patellofemoral articular cartilage abnormalities. Radiology 198: 209–212
3. Lehner KB, Rechl HP, Gmeinwieser JK, Heuck AF, Lukas HP, Kohl HP (1989) Structure, function, degeneration of bovine hyaline cartilage: assessment with MR imaging in vitro. Radiology 170: 495–499
4. Modl JM, Sether LA, Haughton VM, Kneeland BJ (1991) Articular cartilage: correlation of histologic zones with signal intensity at MR imaging. Radiology 181: 853–855
5. Rubenstein JD, Kim JK, Morava-Protzner I, Stanchev PL, Henkelmann M (1993) Effects of collagen orientation on MR imaging characteristics of bovine articular cartilage. Radiology 188: 219–226
6. Erickson JE, Waldschmidt JG, Czervionke LF, Prost RW (1996) Hyaline cartilage: truncation artifact as a cause of trilaminar appearance with fat suppressed three-dimensional spoiled gradient recalled sequences. Radiology 201: 260–264
7. Rubenstein DJ, Kim JK, Henkelman RM (1996) Effects of compression and recovery on bovine articular cartilage: appearance on MR images. Radiology 201: 843–850
8. Lillie RD, Fulmer HM (1976) Histopathologic tectonic and practical histochemistry. McGraw-Hill, New York
9. Benninghoff A (1925) Form und Bau der Gelenkknorpel in ihren Beziehungen zur Funktion. Z Gesamte Anat 76: 43–63
10. Chandnani VP, Ho C, Chu P, Trudell D, Resnick D (1991) Knee hyaline cartilage evaluated with MR imaging: a cadaveric study involving multiple imaging sequences and intraarticular injection of gadolinium and saline solution. Radiology 178: 557–561
11. Adams ME, Matyas JR, Huang D, Dourado GS (1995) Expression of proteoglycans and collagen in the hypertrophic phase of experimental osteoarthritis. J Rheumatol 22 (Suppl 43): 94–97
12. Peterfy CG, Majumdar S, Lang P, van Dijke CF, Sack K, Genant HK (1994) MR imaging of the arthritic knee: improved discrimination of cartilage, synovium, and effusion with pulsed saturation transfer and fat-suppressed T1-weighted sequences. Radiology 191: 413–419
13. Hunziker EB (1992) Articular cartilage structure in humans and experimental animals. In: Kuettner KE, Schleyerbach R, Peyron JG (eds) Articular cartilage and osteoarthritis. Raven Press, New York, pp 183–199
14. Reiser MF, Bongartz G, Erlemann R, Strobel M, Pauly T, Gaebert K, Stoeber U, Peters PE (1988) Magnetic resonance in cartilaginous lesions of the knee joint with three-dimensional gradient echo imaging. Skeletal Radiol 17: 465–471
15. Adam G, Prescher A, Nolte-Ernsting C (1994) MRI of the hyaline knee joint cartilage. Animal and clinical studies. Fortschr Röntgenstr 160: 143–148
16. Monson NL, Haughton VM, Modl JM, Sether LA, Ho KC (1992) Normal and degenerating articular cartilage: in vitro correlation of MR imaging and histologic findings. J Magn Reson Imaging 2: 41–45
17. Paul PK, O'Byrne E, Blancuzzi V, Wilson D, Gunson D, Douglas FL, Wang JZ, Mezrich RS (1991) Magnetic resonance imaging reflects cartilage proteoglycan degradation in the rabbit knee. Skeletal Radiol 20: 32–36
18. Ho C, Cervilla V, Kjellin I, Haghigl P, Trudell D, Resnick D (1992) Cartilage changes in osteoarthritis of the knee. Invest Radiol 27: 84–90
19. Chalkias S, Frezza F, Cova M, Pozzi-Mucelli R, Pozzi-Mucelli M, Dalla-Palma L (1994) Magnetic resonance of the cartilages of the large joints (editorial). Radiol Med 87: 555–573